Th N116 05

# Toward the Limits of Deblending

A.J. Berkhout (Delft University of Technology) & G. Blacquiere* (Delft University of Technology)

## SUMMARY

If we bring sources closer together, they start to `sense' the nearness of each other and their physical behaviour will change. If the separation becomes smaller than half a wavelength, they start to act as one source with new properties (temporal bandwidth, directivity). This fusion process is very complex and nonlinear. To find out whether source fusion has occurred in a blended source array, we image the sources that together form the blended source array. At the same time the deblending concept is extended such that the blending code can be updated simultaneously.
Finally, it is proposed to apply multi-level wavefield encoding to realize an extra attenuation of the residual blending noise.

## Introduction

If we bring sources closer together, they start to 'sense' the nearness of each other and their physical behaviour will change. If the separation becomes smaller than half a wavelength, they start to act as one source with new properties (temporal bandwidth, directivity). This fusion process is very complex and nonlinear. To find out whether source fusion has occurred in a blended source array, we propose to image the sources that together form the blended source array. At the same time the deblending concept is extended such that the blending code can be updated simultaneously. Finally, it is proposed to apply multi-level wavefield encoding to realize an extra attenuation of the residual blending noise.

## Blending performance

Blended acquisition offers the possibility to acquire seismic data with more sources in a shorter survey time (Beasley et al., 1998; Bagaini et al., 2012). To quantify this benefit, Berkhout (2008) introduced the blending performance indicator (*BPI*):

$$BPI = (N'_S/N_S)(T/T'), \tag{1}$$

where $N_S$ refers to the number of sources, $T$ to the survey time and where the accent indicates the blended survey. The *BPI* is the product of two ratios: the source ratio $(N'_S/N_S)$ and the survey time ratio $(T/T')$. Figure 1 illustrates how the *BPI* can be increased by either increasing the source ratio or the time ratio, or by choosing a suitable combination of both. Berkhout and Blacquiere (2013) demonstrated that decreasing the survey time is also a benefit with respect to S/N. This is because less background noise is collected with a smaller survey time ratio. Similar arguments hold for a larger source ratio. In summary: the larger the *BPI* the better. Obviously, there must be limits to how far we can go with increasing the *BPI* while still being able to carry out a successful deblending process. Our research aims at finding these limits of deblending.

## Forward model

The forward model of a blended shot record can be formulated in terms of a matrix-vector equation:

$$\vec{P}' = \mathbf{P}\vec{\Gamma}, \tag{2}$$

where vector $\vec{P}'$ represents a blended shot record. Each element of $\vec{P}'$ is a complex number corresponding to one frequency component of a seismic trace. The columns of matrix $\mathbf{P}$ contain the unblended shot

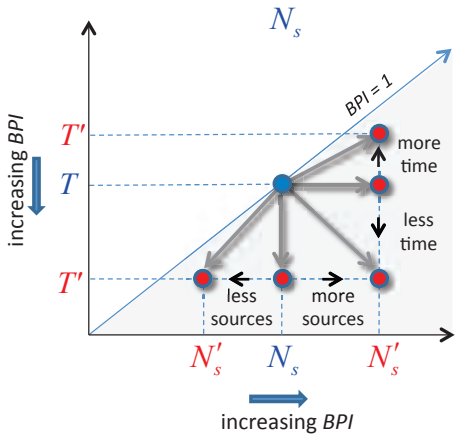


***Figure 1*** *The blending performance can be improved in several ways. A traditional, unblended survey is located somewhere in the upper white area of the graph. A blended survey is located in the lower grey area: the further away from the line BPI = 1, the higher its BPI.*

records, and vector $\vec{\Gamma}$ is the blending operator. The elements of $\vec{\Gamma}$ contain the blending code which may vary from simple time delays to more complex codes. The challenge in deblending is that the problem is underdetermined. This means that physical constraints combined with nonlinear filtering (such as thresholding) must be introduced to transform $\vec{P}'$ into $\mathbf{P}$.

**Pushing the limits of deblending**

Since deblending is an underdetermined problem, the only way to solve it is to bring in additional knowledge. E.g., in many deblending algorithms a mute is applied to the pseudo-deblended (or combed) shot records. Such mute removes seismic energy that can impossibly be attributed to the seismic source of the record being deblended, because of the traveltimes involved. See the example in Figure 2a, where the muting area is indicated. This area can be computed using velocity information. An attractive way to extend this method and to bring in more knowledge, can be realized via the focal transform (Berkhout and Verschuur, 2006). Using macro velocities, focal operators can be constructed that concentrate the data around their focus points. Mathematically the focal transformation can be formulated as:

$$\tilde{\mathbf{P}}' = \mathbf{W}^* \mathbf{P}' = \mathbf{W}^* \mathbf{P} \boldsymbol{\Gamma}, \tag{3}$$

where the focal operator is denoted by $\mathbf{W}^*$ and the tilde symbol denotes the focal domain. By applying the inverse of the focal transform, we return to the original domain: $\mathbf{P}' = \mathbf{W}\tilde{\mathbf{P}}'$, where $\mathbf{W}$ represents the inverse focal operator. In Figure 2b, c and d the results of applying different focal operators to the data are shown. The focal operators are related to different times, ranging from small to large. Notice that the muting areas are different in these figures. They are related to the focal depth. Again, velocity information is required to carry out the focal transform. However, as mentioned this refers to macro-information being routinely available. Actually, looking at equation 3 it is clear that the original blending code $\boldsymbol{\Gamma}$ has now been supplemented with a second code $\mathbf{W}^*$. One could consider the combination of $\mathbf{W}^*$ and $\boldsymbol{\Gamma}$ to be a new blending code. By applying different focal operators, different new blending codes can be realized in a numerical way. We call this *wavefield encoding*. Another interesting property that can be clearly observed in Figure 2 is that the interference between the different blended records is different in each of the wavefield-encoded results. These properties (different mutes, different interferences) lead to the introduction of an extended deblending scheme. It is initiated by our expectation that applying wavefield encoding will result in a better deblending quality when the results of several differently-encoded wavefields are *integrated*. Note that wavefield encoding and decoding are pre- and post-processing steps

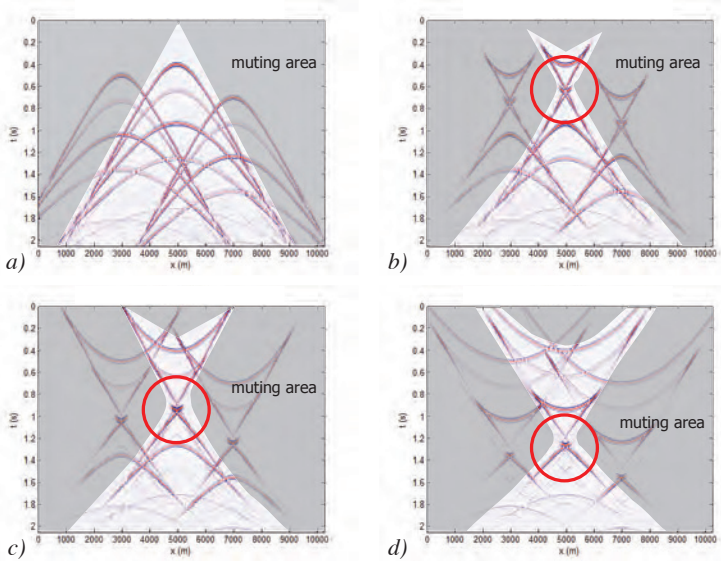


***Figure 2*** *Muting removes 'impossible' energy. a) shows a pseudo-deblended record. In b) to d), wavefield encoding was applied, leading to different muting areas. The red circle indicates the focal area.*

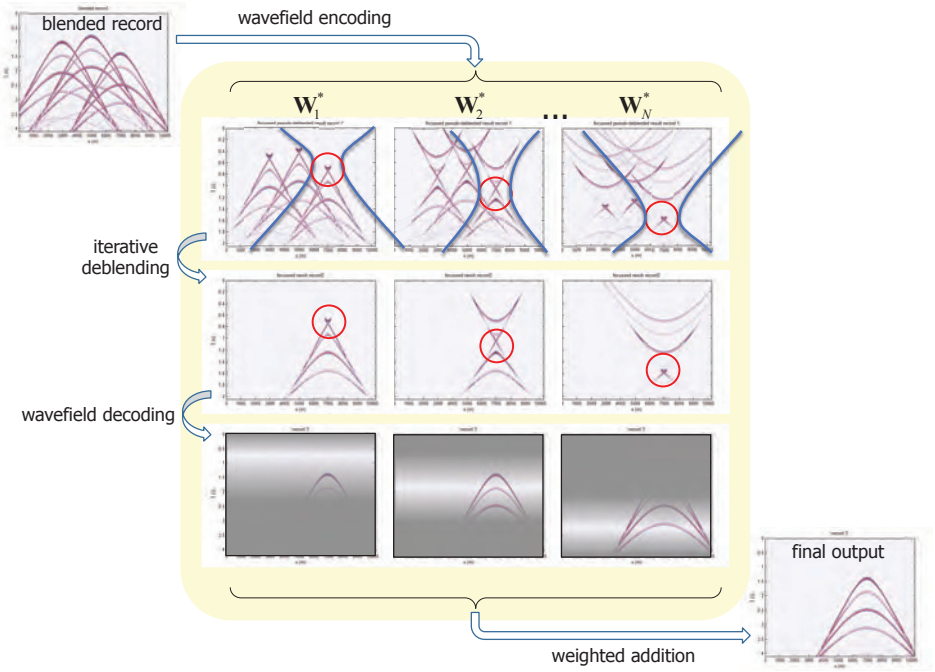


***Figure 3*** *Several deblended results obtained after wavefield encoding are integrated.*

respectively. The actual deblending step can be carried out with any suitable algorithm, i.e., existing deblending methods can be plugged-in. The procedure is visualized in Figure 3 for the situation that wavefield encoding was carried out three times, corresponding to three different focal depths. The interference patterns differ after each of these wavefield encodings and moreover different areas can be muted. It is expected that the best deblending results are obtained around traveltimes corresponding to the focal depth. Therefore, in the integration step the results are weighted to exploit this property.

**Traditional deblending combined with source array imaging**

In our discussion of deblending so far, $\vec{P}'$ and $\vec{\Gamma}$ are given and $\mathbf{P}$ is estimated by minimizing:

$$\left\|\Delta\vec{P}'\right\|^2 = \left\|\vec{P}' - \mathbf{P}\vec{\Gamma}\right\|^2. \tag{4}$$

Although blending vector $\vec{\Gamma}$ is user defined, in practice it may deviate from its pre-specified value, e.g., think of source fusion or phase errors. It is therefore proposed to not only estimate $\mathbf{P}$ from $\vec{P}'$, but to estimate $\vec{\Gamma}$ from $\vec{P}'$ as well. Let us therefore reconsider the model of the blended shot records:

$$\vec{P}' = \hat{\mathbf{P}}\vec{\Gamma}, \tag{5}$$

where $\hat{\mathbf{P}}$ is an estimate of the unblended shot records. Different from equation 2, in equation 5 $\vec{P}'$ and $\hat{\mathbf{P}}$ are given and we need to compute blending operator $\vec{\Gamma}$, using an iterative algorithm that minimizes:

$$\left\|\Delta\vec{P}'\right\|^2 = \left\|\vec{P}' - \hat{\mathbf{P}}\vec{\Gamma}\right\|^2. \tag{6a}$$

The first iteration provides a first-order estimate:

$$\underline{\vec{\Gamma}}^{(1)} = \left[\hat{\mathbf{P}}\right]^H \Lambda\vec{P}', \tag{6b}$$

where $\Lambda$ represents a *diagonal* matrix which scales the deblended shot records, $\underline{\vec{\Gamma}}$ is a band-limited version of $\vec{\Gamma}$, the band limitation given by the seismic bandwidth, and one element $\underline{\gamma}_k$ is referred to as

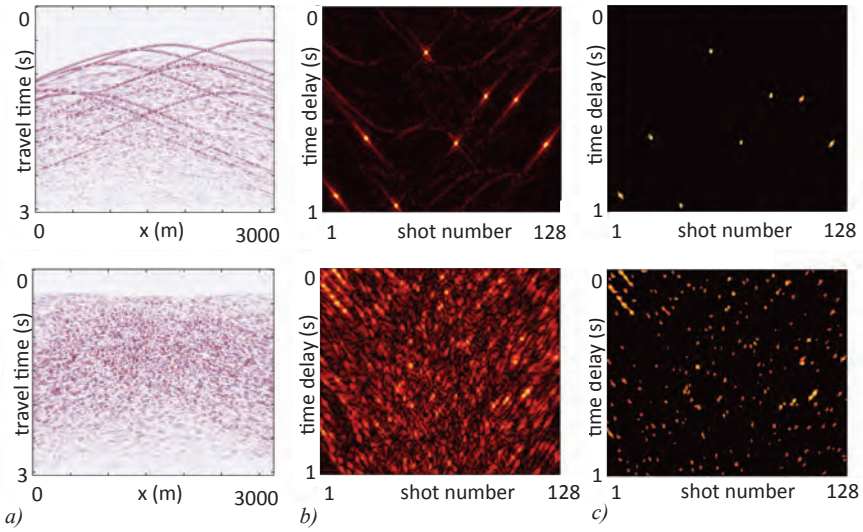


***Figure 4*** *In a) a blended shot record is shown where the array contains 8 sources. The blending codes are time shifts between 0 and 1 s. The corresponding blended source array image is shown in b) for the case that* $\hat{\mathbf{P}} = \mathbf{P}$. *In c) the array image is shown after thresholding.*

the image of the $k^{th}$ source code in the blended array. Figure 4 illustrates the theory. In Figure 4a two blended shot records are shown where the number of sources in the blended source array is 8 and 128 respectively. The blending codes are time shifts between 0 - 1 s. In Figure 4b the blended source array images are displayed, showing the properties of the *individual* sources in the array. In case of 8 sources, they are well separated and no problems are expected in the deblending process. However, in the case of 128 sources, they are much closer together in space and firing time, and it will be difficult to separate these sources. This is particularly true for field data where sources may physically interact in a nonlinear way. If we use field-blended data, the source image will provide valuable information on the *physical* behaviour of blended source arrays. In our current research, imaging of blended arrays is part of the source estimation algorithm in our full wavefield migration package.

## Conclusions

Wavefield encoding creates the opportunity to alter the blending code numerically. By applying wavefield encoding, the results of traditional deblending can be improved. It is proposed to extend the traditional deblending concept by involving the source side in the algorithm as well. This has several advantages: (1) the actual position and the code of the individual sources can be verified, (2) nonlinear interaction between nearby individual sources can be detected, (3) the deblending algorithm can be extended by using a double minimization process: at the detector side and at the source side.

## Acknowledgements

We acknowledge the sponsors of Delphi for the stimulating discussions and their financial support.

## References

Bagaini, C., Hampson, G., Krohn, C. and Moore, I. [2012] Special issue: Simultaneous source methods for seismic data. *Geophysical Prospecting*, **60**(4), 589–590, ISSN 1365-2478, doi:10.1111/j.1365-2478.2012.01093.x.

Beasley, C.J., Chambers, R.E. and Jiang, Z. [1998] A new look at simultaneous sources. *SEG Technical Program Expanded Abstracts*, **17**(1), 133–135.

Berkhout, A.J. [2008] Changing the mindset in seismic data acquisition. *The Leading Edge*, **27**(7), 924–938.

Berkhout, A.J. and Blacquiere, G. [2013] Effect of noise in blending and deblending. *Geophysics*, **78**(5), A35–A38.

Berkhout, A. and Verschuur, D. [2006] Focal transformation, an imaging concept for signal restauration and noise removal. *Geophysics*, **71**(6), A55–A59.